Journal of Spacecraft and Rockets

VOLUME 7 JUNE 1970 NUMBER 6

A Survey and Evaluation of Research on the Discharge Chamber Plasma of Kaufman Thrusters

NELSON L. MILDER
NASA Lewis Research Center, Cleveland, Ohio

Nomenclature

$\mathbf{B}$ = magnetic field strength
$C(\theta)$ = coefficient in Eq. (17)
$\mathbf{E}$ = electric field strength
J_B = beam current
J_N = neutral current (equivalent)
J_i = ion production rate (equivalent current)
j_o = neutral current density
$j_\parallel, j_\perp$ = current densities parallel to and perpendicular to magnetic field
j_+, J_- = beam current density and electron current
k = Boltzmann constant
l = chamber length
l_i = ion mean free path
M = ion mass
N_{coll} = average number of collisions
n_e, n_i, n_o = electron, ion and neutral densities
$P(r,z)$ = ionization probability
$P_{1,2}$ = dimensionless parameters, Eq. (6)
Q_i = maximum ion cross section in Eq. (6)
R = anode radius
$r_c, \bar{r}_c$ = electron cyclotron radius, and rms value
T_e = electron temperature
U_i = ionization potential
U_l = excitation potential
$V(r)$ = plasma potential
$\bar{V}_-$ = mean thermal energy
ΔV_r = radial plasma potential difference
$\bar{v}_i$ = ion speed
W = atomic mass, amu
ϵ_a = electron anode loss, ev/ion
ϵ_b = discharge loss, ev/beam ion
ϵ_c = collisional loss, ev/ion
ϵ_h = electron wall loss, ev/ion
ϵ_t = discharge loss ev/plasma ion
η_{nom} = nominal propellant utilization efficiency
ν_{ee}, ν_{en} = electron-electron and electron-neutral collision frequencies
ν_i = ion production rate
$\Sigma_{m,p}$ = ionization coefficients
σ_0 = zero field conductivity
σ_+ = ionization cross section
ϕ = ratio of beam current to total current to screen
τ = mean collision time
ω = ratio of total ion current to beam current
ω_e = electron cyclotron frequency

Introduction

SINCE its introduction in 1960,[1] the mercury bombardment ion thruster has been the subject of extensive research and development programs. Bombardment thrusters have been operated with ion chambers ranging in diameter from 2.5 cm² to 150 cm.[3] The marked success of these programs is evident, i.e., from Table 1, which shows a comparison between the performance levels of the first thruster concept[1] and the recent SERT II thruster module.[4,5] Improvements in performance have been primarily the result of experimental optimization. For example, improved permanent magnet design[6] has eliminated the need for power consuming electromagnets. Cathode life has been significantly extended by replacing refractory metal cathodes by oxide-coated emitters.[7,8] Because of its ability to withstand exposure to air after ground testing of flight hardware, the hollow cathode design[9] is presently being used in SERT II thrusters. Discharge power consumption has been substantially reduced by improvements in ion extraction concepts[5,10] as well as by using optimized magnetic field configurations.

Understanding of the physical processes governing thruster performance has not kept pace with experimental progress for two reasons. First, up to the present time laboratory experience and calculations using simple theoretical approximations have sufficed to lead to major increases in thruster performance. Second, and probably of greater significance, the complex physical processes are so strongly coupled in the discharge plasma that their experimental isolation and measurement has proved to be exceedingly difficult. The purpose of this paper is to survey and evaluate the present understanding of the physics of the discharge chamber. Ideally, an accurate theoretical model of the discharge pro-

Nelson L. Milder has been a physicist with NASA Lewis Research Center since 1961, when he received his Master of Science degree in physics from Ohio State University, Columbus, Ohio. He has been primarily engaged in theoretical and experimental research in electric propulsion and plasma physics. His publications include a range of subjects associated with ion thruster technology and the physics of the discharge plasma in such thrusters. He is a member of the AIAA.

Presented as Paper 69-494 at the AIAA 5th Propulsion Joint Specialist Conference, U.S. Air Force Academy, Colo., June 9-13, 1969; submitted June 4, 1969; revision received January 26, 1970.

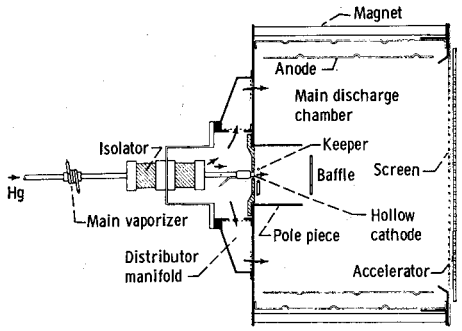

Fig. 1 Section view of SERT II thruster.[13]

cess could lead to further significant improvements in thruster design and performance.

Electron Bombardment Ion Thruster

Vaporized mercury, generally introduced at the upstream end of the thruster, is ionized in the chamber (Fig. 1) by means of electron bombardment.[11-13] The electrons are provided by a cathode and gain sufficient energy for ionization from the cathode-anode potential difference. Present mercury thruster designs use an axially symmetric diverging magnetic field to inhibit electron flow to a cylindrical anode. The sources of these electrons are the cathode emission and secondary electrons released in the ionization process. The primary (or cathode) electrons lose energy and are redistributed as a result of inelastic ionizing and exciting collisions with mercury atoms. Some of the primaries escape across the magnetic field to the anode without suffering any inelastic collision. As a result, the electron distribution in the ion chamber is generally non-Maxwellian.

Ions are extracted from the chamber by means of a grid system. The sheath at the plasma-grid boundary sustains the electric field necessary to direct ions into the beam. The characteristics of this sheath depend upon grid geometry, plasma density, electron temperature, and the nature of the electron and ion charge distributions within the plasma and sheath regions.

There also are sheaths at all boundaries between the plasma and the thruster components (the anode, cathode, chamber wall, and in the case of the more recent thruster configurations,[3,7] at pole piece surfaces and the hollow cathode baffle). These sheaths strongly couple to the plasma and thus greatly affect plasma characteristics.

The discharge energy supplied to the thruster is consumed in several ways. Ionization and excitation of the mercury propellant result from inelastic collisions with electrons. The plasma in the ion chamber is optically thin (radiation is not appreciably readsorbed by the plasma) so that excited atoms and ions in the plasma lose energy by radiation. Wall recombination is also responsible for a large fraction of energy consumption.[14] In this process ions produced in the plasma volume are accelerated to chamber walls by potential gradients in the plasma and in plasma sheaths. Also, the recombined neutral particles leaving the walls have a definite probability of being reionized or excited, hence absorbing

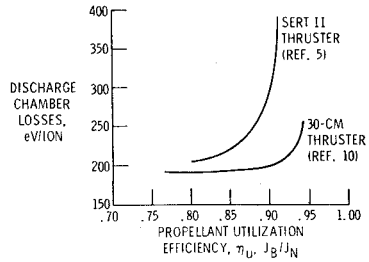

Fig. 2 Ion production costs vs propellant utilization.

Table 1 Comparison of thruster performance between first thruster and present SERT II module

	First thruster[2]	SERT II[4,5]
Cathode power, w	40	27
Magnet power, w	180	0
Beam power, w	500	750
Estimated cathode life, hr	50	10,000
ev/beam ion	1250	250–300
Thrust level, mlb	1.0	6.2
Propellant utilization, %	80	85
Over-all power efficiency, %	27–33	86

additional discharge energy. Finally, plasma (secondary) electrons, randomized primary electrons and primaries which have no particle encounters thermally dissipate their kinetic energy at the anode.

Other mechanisms for energy consumption, such as electron-plasma wave interactions, two-stream and other hydromagnetic instabilities and plasma turbulence may exist. Although low-frequency disturbances (of the order of several kilohertz) have been observed in bombardment thrusters,[15] little is known about their origin at present.

Ion chamber performance characteristics are typically displayed as shown in Fig. 2. Here ion production cost (in electron-volts of energy required per beam ion produced) is plotted as a function of propellant utilization efficiency, J_B/J_N, the ratio of beam current to total propellant flow expressed as an equivalent current. In general, such curves have a relatively flat, or linear, portion at low utilization efficiency, rising rather steeply at high propellant utilization efficiency.

Theoretical Models of the Plasma Discharge

The principal theoretical approaches are summarized in Table 2. Most of the important plasma processes and potential problem areas were recognized in Kaufman's[1] pioneering work. Simple continuum equations of a fully ionized, two-component plasma were used to describe the steady-state motion of electrons across a uniform magnetic field. Ion and neutral equations of motion were neglected, and the resulting expression for electron current density components parallel and perpendicular to the uniform magnetic field were obtained

$$\mathbf{j}_{\parallel} = [\sigma_0/(1 + \omega^2\tau^2)]\mathbf{E} \tag{1}$$

$$\mathbf{j}_{\perp} = [-\omega\tau\sigma_0/(1 + \omega^2\tau^2)]\mathbf{E} \times \mathbf{B}/|\mathbf{B}| \tag{2}$$

where $\mathbf{j}_{\parallel}$ is the current density parallel to the magnetic field, $\mathbf{j}_{\perp}$ is the current density normal to the uniform magnetic field, σ_0 is the zero-field conductivity, ω is the electron cyclotron frequency, τ is the time per collision, $\mathbf{E}$ is the electric field and $\mathbf{B}$ the magnetic field. The importance of minimizing the radial potential gradient to minimize ion flow to the chamber walls was recognized. From Eq. (1) an approximate expression for this gradient has the form

$$\Delta V_r \approx 10^{11} J_- \bar{V}_-^{1/2}/\pi n_e^2 r_c^2 \sigma_+ R \tag{3}$$

where ΔV_r is the radial potential difference, J_- is the electron current, $\bar{V}_-$ is the electron thermal energy in volts, n_e is the plasma density in cm^{-3}, r_c is the electron cyclotron radius in cm, $\sigma_+(cm^2)$ is the ionization cross section, and R is the chamber radius. Consideration also was given to cross-field diffusion. The average number of primary electron collisions occurring in the diffusion process is

$$N_{coll} \approx (R/r_c)^2 \tag{4}$$

This analysis resulted in order-of-magnitude calculations sufficient for the initial thruster designs. However, spatial variation of plasma parameters in the discharge cannot be

accurately assessed from such calculations. Kohlberg[16,17] presented a calculation based on the collisional Boltzmann equation[18] to determine whether the electron distribution is established by a "weak" plasma or "strong" plasma condition. The weak plasma condition presumes that electrons establish a steady-state distribution by means of electron-neutral atom collisions. The strong plasma condition presumes that electron-electron collisions dominate. The calculation begins with the assumption of a weak plasma and shows that the electron distribution depends on local properties of the electromagnetic field as well as on the electron-neutral collision frequency. From this model an electron temperature is derived which varies as B^{-2}. Because of the fact that this variation was not observed experimentally and that the experimentally determined electron temperatures were about a factor of three below calculated values, Kohlberg concluded that the electron distribution was established by the strong plasma condition,

$$\nu_{ee} \gg \nu_{en} \tag{5}$$

where ν_{ee} is the electron-electron collision frequency and ν_{en} the electron-neutral collision frequency. These collision frequencies are those for momentum transfer only. In addition, radial profiles of plasma density and potential were calculated from continuity equations. These calculations were found to approximate experimental probe measurements for plasma densities of the order of 10^{11} cm^{-3}.

Kaufman[19] returned to the problem and presented a method for scaling gross performance characteristics, based upon a consideration of over-all discharge performance curves (Fig. 2). A rough performance correlation was effected by defining a nominal propellant utilization η_{nom} in terms of the minimum ev/ion, and obtaining expressions for $(\text{ev/ion})_{\text{min}}$ and η_{nom} in terms of dimensionless parameters;

$$P_1 = j_o l_i Q_i W(\bar{r}_c/R)^2,\ P_2 = j_+ l_i Q_i W \tag{6}$$

where j_o is the neutral current density, l_i the ion chamber length, Q_i the maximum first ionization cross section (in units of $\pi a_0^2 = 0.88 \times 10^{-16}$ cm^2), W the atomic mass in amu, $\bar{r}_c$ the electron cyclotron radius for an rms secondary electron speed, R the ion chamber radius and j_+ the ion beam current density. Measurements of $(\text{ev/ion})_{\text{min}}$ and η_{nom} for a variety of source geometries and operating conditions can be correlated when plotted against P_1 and P_2. Because of the multitude of approximations and assumptions required to yield concrete relations between variables, the resulting correlation was accurate only to within $\pm 50\%$ on $(\text{ev/ion})_{\text{min}}$ and about $\pm 20\%$ on the calculation of η_{nom}.

Masek,[20] Knauer,[21] and Cohen[22] presented analyses based upon more detailed considerations of hydromagnetic equations of motion than used in the Kaufman analyses. The problems studied differed from one another, although the fundamental physical considerations were similar. Masek sought to obtain expressions for the potential gradients and ion fluxes in the plasma. Ion mobility as well as electron mobility and collisional diffusion were included. The difficulty here rests with the long ion mean free path for momentum transfer collisions. This situation led to expressions involving an indeterminant ion mobility coefficient. Using measured density profiles and estimating the value of the ion mobility, it was possible to obtain reasonable agreement between measured and calculated density profiles in some cases.[20]

In Knauer's analysis an attempt was made to derive the appropriate equations for the plasma density distribution and energy balance, as well as to apply the analysis to deriving thruster scaling criteria.[21] Collisional diffusion of electrons across the magnetic field to the anode was considered as the dominant process in establishing the plasma radial density profile. An attempt was made to include a spatial electron temperature distribution and an average inelastic collision

Table 2 Theoretical models of the plasma discharge in a Kaufman thruster

Author	Analytical approach	Comments
Kaufman[1] (1960)	Continuum equations of a fully ionized plasma. Approximate analysis of the inelastic collision processes.	Simplest analytical approach. Recognized most of the major problems, although did not analytically assess them.
Kohlberg[16,17] (1963)	Uses plasma kinetic equation to obtain form of the electron distribution function. Includes momentum transfer collisions only. Ionization rate included in electron continuity equation from which radial plasma density and potential are calculated.	Analysis uses microscopic approach. Assumptions and approximations required limit applicability. Neglects primaries and ion motion in plasma volume, magnetic field divergences, excitation collisions.
Kaufman[19] (1965)	Evaluate over-all source performance in terms of minimum ev/ion and propellant utilization at twice minimum ev/ion. Derived dimensionless correlation parameters [Eq. (16)]. Bohm criterion for ion directed velocity.	Expands somewhat on simple analysis used in Ref. 1, but requires many assumptions to make problem tractable. First attempt to directly incorporate experimental performance data in a theoretical model.
Masek[20] (1966)	Hydromagnetic continuum equations including momentum transfer collisions only, ideal gas law as equation of state, and second order ion drift in ion mobility. Equation for ions and Maxwellian electrons used to solve for current fluxes in cylindrical coordinates.	Some agreement between measured potential profiles and theory for certain operating conditions. Density distribution from experiment. Neglects primary electrons, magnetic field divergences. No explicit inclusion of excitation and ionization processes in plasma eqs.
Cohen[22] (1966)	Stability analysis of Kadomtsev and Nedospasov specialized to case of radial electric field with azimuthal perturbation in potential and density. Hydromagnetic equations of motion for ions, electrons, plus continuity equations used to calculate currents. Calculation of anomalous electron loss across uniform magnetic field.	Calculates effect of instability growth on anomalous electron transport in bombardment thruster (e.g., theory applied to special problem). Ionization by primaries neglected; nonuniformities in magnetic field neglected. Obtains good agreement with measured critical magnetic field.
Shaw[26] (1966)	Boltzmann-Vlasov equation used to obtain general steady-state continuity and momentum conservation equations for three-component plasma (ions, primary and Maxwellian electrons), with numerical techniques required to solve equations. One dimensional, concentric cylindrical symmetry, uniform magnetic field (axial) and uniform electron temperature assumed.	Includes effect of ion acceleration in electric field in a tractable way. Represents a one-dimensional approximation to actual thruster plasma. Experimental correlation between measured thruster densities and theory of same order as other analogous approaches.
Knauer[21]	Hydromagnetic continuum equations including spatial variation of electron temp. through energy equations. Continuity equations including average ionization rates. Radial electron drift from collisional diffusion.	Theory sketchy and difficult to assess accurately. Contradictions in current derivations, but introduces some interesting analytical concepts for macroscopic approach to thruster performance calculations. Attempts to use power balance equations to derive expressions for density distribution.
Masek[25] (1969)	Semiempirical calculation of ion currents using Bohm criterion. Calculation of volume ion production costs for Maxwellian and primary electrons. Comparative calculations of energy consumed per beam ion from volume costs. Electron anode loss calculations.	Model can be used to calculate thruster performance characteristics from plasma parameters. Depends on accurate Langmuir probe data. Probably most useful approach to date to understanding discharge energy losses. Semiempirical approach. Depends on measured electron temperatures and densities.

frequency. The complexity of the problem was expanded to require a consideration of the distribution of arc power supplied to the plasma. Unfortunately, simplifications introduced to make the problem tractable led to certain inconsistencies in the analysis. For example, the diffusion coefficient used presumes a uniform electron temperature, but the final expression for electron current incorporates a spatial temperature variation.

Cohen[22] specialized the hydromagnetic stability theory of Kadomtsev and Nedospasov[23] for the discharge plasma; in particular, the direction of the applied electric field became radial rather than axial (as in the positive column). In this theory, the growth of an azimuthal perturbation on the electric field produced large electron losses to the anode. These losses exceed by several orders of magnitude the losses predicted by collisional diffusion theory. This excessive electron flow is termed "anomalous" diffusion in the literature. Some experimental evidence[15,24,25] indicates that anomalous diffusion may occur in the mercury thruster.

A theoretical treatment of one-dimensional, low-pressure plasma discharges has been applied to the Kaufman thruster by Shaw.[26] The analytical approach is comparable in certain respects to the analyses of Kohlberg[17,18] and Masek.[20] The Boltzmann-Vlasov[27] form of the plasma kinetic equation is used to derive equations of continuity and momentum conservation for a three-component plasma consisting of ions, primary electrons and Maxwellian electrons. In some respects the calculations are more comprehensive than those of Kohlberg and Masek in that a complete set of plasma component equations, including the effect of ion production, are solved for the plasma parameters. In addition, the effect of the long ion mean free path is included in a more tractable way than in Masek's work. The equations represent a one-dimensional approximation to the actual thruster configuration. Numerical methods are required in order to obtain solutions that can be correlated to experiment.

Shaw's analysis yields reasonable agreement with the measured radial ion and Maxwellian electron density distributions.[28] Poor correlation is obtained between the measured and calculated primary electron density distributions. Although this lack of correlation was attributed in Ref. 26 to a lack of one-dimensional symmetry in actual thruster configurations, it may well be the result of the approximations used in deriving one-dimensional continuum equations for the primary electrons. It is of interest to note that in the general approach used in Shaw's work, the only elastic collisions considered important are electron-neutral and possibly ion-neutral collisions. This is in opposition to Kohlberg's result given by Eq. (5), that electron-electron Coulomb collisions must dominate the low pressure discharges of bombardment thrusters.

The most recent approach, by Masek,[25] is essentially a semi-empirical analysis. This work and that of Knauer et al.,[21] represent the most comprehensive Langmuir probe studies of bombardment thruster plasmas reported to date. Rather than start with microscopic equations of motion (as did Kohlberg and Shaw) or macroscopic equations (as did Masek,[20] Kaufman[1,19] et al.), Masek uses current flux, ion production and energy balance calculations to determine thruster performance. These calculations provided reasonably accurate phenomenological descriptions of the two oxide-cathode thrusters (15 cm diam and 20 cm diam) investigated. Various phenomena such as ion and electron wall losses, ion production cost (in electron volts per plasma ion produced) and beam extraction efficiency were determined in several different ways. The results of the different approaches were then compared and were found to be in general agreement. The analysis used required detailed probe measurements of such plasma parameters as ion and electron densities and electron temperature as functions of location in the chamber. Such measurements are quite tedious to obtain and would be subject to the characteristics of the specific thruster configuration investigated. This is the most important limitation to generalizing the approach to an arbitrary thruster configuration. In estimating over all thruster performance the essential relations required are between the beam current and the grid extraction system,

$$J_B = \phi J_i \tag{7}$$

and between the volume ion production cost (ev/plasma ion) and the cost to produce a beam ion (ev/beam ion),

$$\epsilon_B = \omega \epsilon_i \tag{8}$$

Here J_B is the beam current, ϵ_B the beam ion production cost, and J_i is the Bohm current[28] to the extractor grids determined from the relation

$$J_i = \sum_j (n_i v_i)_j A_j \tag{9}$$

where A_j is a concentric element of extraction grid area. The ion density n_i and speed v_i are determined from probe measurements of density and electron temperature, respectively, for each area element. The parameter ϵ_i is the volume ion production cost. The parameter ϕ is the fraction of the total Bohm current to the screen grid that goes into the extracted beam. This fraction is nearly equal to the fraction open area of the screen. Also, ω is the ratio of the total ion current in the ion chamber (i.e., current to the walls plus beam current) to the beam current. The concept of using the Bohm criterion (i.e., that the ion speed at a sheath edge is that corresponding to a kinetic energy equal to one-half the electron temperature) to calculate ion current to the walls was initially introduced in thruster analysis by Kaufman.[1] At that time, however, the required measurements of plasma density and electron temperature near a wall were unavailable. This particular model of the discharge will be further considered in other sections of this paper.

To summarize, existing theoretical models of the discharge have been primarily directed toward calculating certain plasma parameters (such as radial plasma density and potential distributions and particle flux in the plasma volume). The success of these models in predicting thruster performance has been very limited. The general approaches have included models based on kinetic equations of motion (microscopic) and the hydromagnetic continuum equations of motion (macroscopic).

Discussion

For convenience, the discussion is divided into five specific areas. This division is somewhat artificial, since coupling between various phenomena in the real problem is generally quite strong.

Electron Distribution in the Ion Chamber Plasma

There are at least two important reasons for seeking a detailed knowledge of the electron distribution in the discharge chamber. First, in the bombardment thruster collisions between mercury atoms and primary electrons and electrons in the Maxwellian "tail" produce ionization. In Ref. 28, it was concluded that the primaries are one to two orders of magnitude more effective in ionizing mercury than are the high energy Maxwellians. Thus, from the viewpoint of producing more uniformity in distribution to reduce grid erosion[29] (and possibly radial potential gradients), a uniform distribution of primaries is desirable. Second, the electron distribution determines other plasma characteristics. For example, electron temperature, plasma potential and ion production depend on the electron distribution. The potential distribution affects the ion flow to chamber walls and the beam extraction system. The ion production and current flow in turn strongly influence such thruster parameters as

propellant utilization and discharge energy consumption per beam ion produced.

The first Langmuir probe measurements of the electron distribution in the plasma of a Kaufman bombardment thruster were reported by King and Kohlberg[18] and simultaneously by Strickfaden and Geiler.[28] The latter researchers associated the non-Maxwellian nature of the probe voltage-current characteristic with a monoenergetic distribution of high energy electrons (primaries) superimposed upon a low energy Maxwellian distribution. (Such double distributions had been observed earlier by Medicus[30,31] in neon fireball discharges.) When plotted semilogarithmically, the current-voltage characteristics are as shown in Fig. 3 (see Ref. 32). It is seen that subtracting the primary electron contribution from the actual probe trace yields the characteristic linear slope on the corrected curve. The hypothesis that there are two distinct populations is often a simplification of the actual distribution. Under some operating conditions, the observed probe characteristics are not amenable to this simplification.[21] Inelastic and elastic collisions produce a spread in the primary energy.

Experimental determination of the actual energy distribution would involve measurements of the second derivatives of Langmuir probe characteristics.[33] In general such measurements are tedious and inaccurate, although Medicus[34] has presented a graphic technique that simplifies the measurement. The method is based on the fact that the current to a small probe is produced by electrons with kinetic energies equal to or greater than the electron-retarding probe potential. Tangents are constructed to the probe current-voltage characteristic near the "knee" of the curve corresponding to the plasma potential. It is shown in Ref. 34 that the electron energy distribution $g(U)$ is given by a relation of the form

$$g(U) \sim U^{-1/2}\Delta j_o/\Delta U \tag{10}$$

where Δj_o is determined by the intersection of two adjacent tangents with the current axis of the current-voltage characteristic, ΔU is the voltage increment corresponding to the two tangent lines intersection with the probe characteristic, and U is the probe voltage at the center of the voltage increment ΔU. The procedure requires very accurate measurements of the probe characteristic. Further study is required to determine whether this technique could be applied to thruster discharges. Probe measurements have, however, yielded much useful information concerning the nature of the distribution. Probe current-voltage characteristics (Fig. 3) have been used to determine local primary and Maxwellian electron densities as well as local electron temperature and plasma potential in operating ion thrusters. From such measurements it has been concluded that, on the average, the ratio of primary to Maxwellian electrons for mercury thrusters generally is of the order of 0.1 or less.

Excitation and Ionization Processes in the Chamber

The most recent attempts to assess the effect of ionization and excitation processes on thruster performance have been based on the volume ion production cost calculations of Dugan and Sovie.[35] A method was presented for calculating the energy costs to produce an ion in low density (tenuous) plasmas, such as are found in thrusters. Here the Gryzinski[36,37] semiclassical calculation of the cross section for inelastic electron-atom collisions was used. This theory presumes that the inelastic electron-atom collision can be treated as a classical two-body encounter between the incident and bound electrons. The method yields ionization cross sections that are in good agreement with experimentally measured values.

In order to obtain excitation cross sections the Gryzinski calculation was modified in Ref. 35 to account for quantum mechanical effects associated with the bound electronic configuration of excited states. In particular, certain computational rules were introduced to account for allowed and forbidden transitions as well as for different electron spin states. The excitation cross sections obtained by this method were then used to obtain volume ion production costs in helium, argon and cesium plasmas. Two cases were considered, assuming 1) a pure monoenergetic electron beam impinging on a cold background gas, and 2) Maxwellian electrons interacting with the neutral gas. For the latter case, the ion production cost is given by

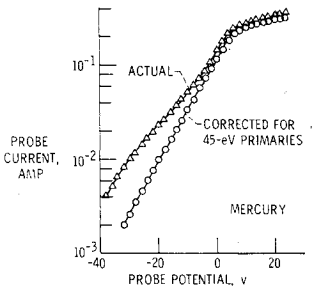

Fig. 3 Typical Langmuir probe semilog plot for mercury plasma in a thruster.[32]

$$\text{volume ion cost (ev/ion)} = \text{ionization potential} + \frac{\sum(\text{excitation coefficients})}{\text{ionization coefficients}} \tag{11}$$

where the summation on the right side is over the excitation coefficients to all possible excited states of the atom. These coefficients were obtained by averaging the calculated excitation cross sections over a Maxwellian electron energy distribution.

Dugan and Sovie presented a general two-level (ground state plus an average excited state) atom theory for the Maxwellian case which is of particular importance for mercury bombardment thrusters. The theory enables calculation of the volume ion production cost for any atomic species. The average excited state can be obtained once the ionization potential and first excited state energy are specified. Atoms for which the ratio of the first excited state energy to ionization energy is less than 0.45, are assigned a mean excited state energy equal to the energy of the first excited state. For values of this ratio greater than 0.45, the mean excited state energy is taken to be the average of the ionization and first excited state energies.

Mickelsen[38] has used the theory to discuss the volume ion production costs for mercury. Figure 4 shows the normalized ion generation loss plotted against the ratio of first excitation potential U_l to ionization potential U_i. An estimate of the minimum volume ion production costs for a typical Maxwellian mercury plasma of the bombardment thruster can be obtained from the figure. Assuming an electron temperature of about 5 ev, and excitation energy of about 4.7 ev and an ionization potential U_i equal to 10.4 ev, the value of

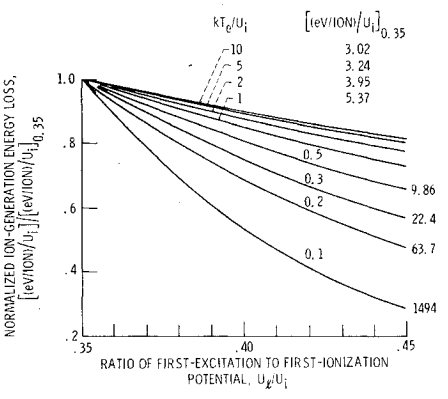

Fig. 4 Normalized ion-generation energy loss calculated from a general-atom theory.[35,38]

the parameter kT_e/U_i is about 0.5 and the value of U_l/U_i is about 0.45. The normalized ion-generation energy is 0.7. The value of $(\text{ev/ion}/U_i)_{0.35}$ to be used is 9.86, so that (ev/ion) is 72 ev/ion. This value is approximately 2.5–3 times smaller than the best measured ev/beam ion in mercury bombardment thrusters, indicating the existence of other modes of energy consumption in the ion chamber.

Based on the procedure of Ref. 35, ion production rates and energy costs per mercury ion resulting from inelastic electron-atom and electron-ion collisions were calculated by Masek.[25] Assuming that ionization occurs only from the ground state the volume ion production rate is given by the expression,

$$\bar{\nu}_i = n_o[n_m\Sigma_m + n_p\Sigma_p](\text{ions})/\text{sec-cm}^3 \qquad (12)$$

where n_o is the local neutral mercury atom density, n_m the local Maxwellian electron density, and n_p the local primary electron density. The ionization coefficients Σ_m for Maxwellian electrons and Σ_p for primaries are obtained by averaging over experimental ionization cross sections.[20] The densities n_m and n_p were obtained from probe measurements. Because accurate measurements of neutral density in the discharge chamber are not available, n_o was calculated from the mass continuity equation. Calculation of the ion production rates for each term of Eq. (12) showed that primaries play a major role in the ionization process. In addition, Masek calculated the energy cost to produce a plasma ion using the locally measured primary and Maxwellian electron densities and the procedure outlined in Ref. 25. The results of this calculation are shown in Fig. 5, where ϵ_c' is the local (position dependent) collisional loss. The total collision loss would require averaging over the entire plasma volume. It should be noted from the figure that for an electron temperature of 5 ev, the local collisional loss is about 50 ev/ion. The ~25% discrepancy between Masek's value and Mickelsen's[38] calculation (Fig. 4) is probably due to the difference between calculated excitation cross sections used to obtain Fig. 4 and the experimental single transition cross sections used in obtaining Fig. 5. In the latter figure ion excitation is included and is significant only for primary electrons. The curves of Fig. 5 are based on the assumption that the ground state ion and neutral populations are equal. The figure also illustrates the fact that primary electrons can have a major role in the ionization process. (This conclusion is valid only for mercury bombardment thrusters. Probe measurements in cesium bombardment thrusters[20] reveal the absence of primary electrons in the discharge plasma. Ionization occurring in the plasma volume of cesium thrusters is due to collisions with Maxwellian electrons only. The analysis of such thrusters is a unique problem in itself and is thus outside the scope of the present study.)

Discharge Energy Required to Produce a Beam Ion

So far we have considered the discharge energy costs required to produce a plasma ion by means of collisions with electrons. If no other energy loss mechanisms prevailed, and if all plasma ions could be extracted as beam ions, then the ev/ion calculations of the preceding section would also be indicative of energy costs to produce a beam ion. Unfortunately, other loss mechanisms do exist. Calculations of discharge energy losses from a consideration of basic plasma processes should be one of the major objectives of a theoretical (or semiempirical) model of the discharge. Some of these additional loss processes include radiation losses, wall recombination, anomalous electron loss to the anode and charge exchange losses at the grid extraction system.

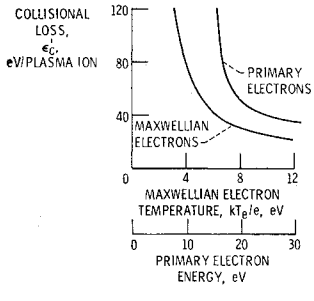

Fig. 5 Local collisional energy loss factor.[25]

In the preceding section radiation losses were accounted for by de-excitation of atoms to the ground state. As was indicated earlier, the plasma is optically thin and essentially all the radiation escapes from the plasma volume. However, metastable states of the atom with lifetimes of the order of milliseconds could return to the ground state by means of collisions with other Hg atoms or through resonant energy transmission with a foreign atom. In addition, collisions between electrons and metastable mercury atoms could contribute to the volume ion production cost. Dugan and Sovie[39] have studied electron collisions with metastables in tenuous helium plasmas. Again, the Gryzinski method for calculating cross sections was used. It was found that the ionization from metastable states had an unexpectedly small effect on the volume ion production costs. This was attributed to the small cross section for ionization as compared to the excitation cross sections for these states. To date no similar study has been made on mercury thruster plasmas.

Potential gradients within the plasma and plasma sheaths accelerate the ions to the walls of the discharge chamber. Upon reaching the walls, ions recombine with electrons to form atoms and release kinetic energy, eventually desorbing from the walls as lower energy neutrals. Masek[25] has used locally measured plasma densities and electron temperatures in conjunction with an ion speed derivable from Bohm criterion

$$\bar{v}_i \geq (kT_e/M)^{1/2} \qquad (13)$$

to calculate these ion currents. The ion currents to the walls determined in this manner were used to obtain the fraction of the total ion current produced in the chamber that becomes beam current [equivalent to ω^{-1} of Eq. (8)]. Masek found this fraction to compare favorably with a corresponding value determined from the ratio of measured beam current to calculated total ion production rate. [The total ion production rate was computed by summing the local ion production rate from Eq. (12) over the total discharge chamber.] A comparison of the two ratios is given in Table 3.

According to Masek's work, the major discharge energy consumption occurs as a result of inelastic collisions. From Fig. 5, the energy cost for 30 ev primaries and 5 ev Maxwellians is about 80 ev per plasma ion. The total energy cost per plasma ion is

$$\epsilon_t = \epsilon_c + \epsilon_a + \epsilon_h \qquad (14)$$

where ϵ_c is the collisional energy cost, ϵ_a is the energy cost resulting from electron loss to the anode and ϵ_h is the electron energy loss to the chamber walls. The losses ϵ_a and ϵ_h are

Table 3 Comparison of ion flux and ion production rate calculations for a 15-cm thruster[25]

	Total discharge chamber ion current, amp	Beam current amp	Ratio of beam to ion current, ω^{-1}
Determined from probe data	3.79	0.5	0.13
Calculated from Eq. (1) and summing over chamber volume elements	4.5	0.55	0.12

calculated to account for about 20% of the total volume ion production cost. These factors, coupled with the fact that for a 15-cm-diam thruster wall losses [the factor ω in Eq. (8)] resulted in an ion extraction efficiency of about 13% led to a value of energy cost per beam ion ϵ_B of about 800 ev/ion.[25] Since the present SERT II thruster configuration has an ev/ion of about 250–300, and if ϵ_t remains about the same, then the ion extraction efficiency may be of the order of 30–50%. This conclusion is in agreement with Masek's data for a 20-cm-diam thruster.

The anomalous electron loss to the anode discussed in Ref. 22 may occur in bombardment thrusters and may be a function of the magnetic field configuration. For a uniform axial magnetic field, a critical field strength for the onset of the anomalous diffusion phenomenon can be calculated.[22] It appears that thruster operation at approximately uniform field strengths near this critical value effectively reduces this energy loss to a minimum.[15,22] This effect has also been noted for the highly divergent fields used in SERT II thrusters.

Loss of beam ions as a result of charge exchange has a negligible effect on ev/ion calculations in comparison to previously described losses. The physical process occurring consists of a charge exchange between thermal neutrals in the ion extraction region and high energy ions. The resulting charge exchange ion can strike a grid surface and thus be lost to the beam. The probability of its striking a surface (rather than escaping as a beam ion) depends on the grid system design as well as the spatial location of the charge exchange process.[40] Present extraction system designs and operation at high propellant utilization efficiency have combined to minimize this energy loss process.

Based on this survey, it appears that the major energy loss occurs from wall recombination. Anomalous or enhanced electron losses can be minimized by operating at the appropriate magnetic field strength. Further gains in minimizing discharge energy costs per beam ion will thus require thruster designs that use an effectively reduced wall surface area and improved ion extraction systems. Because of the unavoidable volume ion production costs, future improvements may be not much greater than two or three.

Propellant Utilization Efficiency

The dependence of discharge energy loss on propellant utilization efficiency for a typical thruster was shown in Fig. 2. It is noted from such curves that a sharp rise in discharge losses occurs at high utilization efficiencies. This phenomenon is common to all thruster configurations. It is due primarily to the fact that ion density levels off as utilization increases. The discharge current, however, must be increased to produce increased utilization. This increase in electron flow enhances the electron anode loss and electron temperature (and thus ion losses to the wall).[25] The net effect is thus a sharp rise in discharge energy loss.

Several factors affecting propellant utilization in bombardment thrusters such as electron distribution, ion production rates and ion flux to walls have been discussed in preceding sections of this paper. A major unknown factor in ionization calculations is the neutral density in the chamber. This density is a function of propellant flow rate and neutral efflux from ion chamber wall surfaces. Recently, preliminary measurements have been made of the mean neutral atom speed in a bombardment thruster.[41] A velocity selector and ion gage detector were used to measure the average speed of the neutral atom efflux through a small hole drilled in the chamber wall. Calculations based upon these measurements indicated neutral atom temperatures may be about 1000°K. Generally neutral density calculations assume a neutral temperature equal to the wall temperature of about 500–600°K. The effect of a higher neutral temperature on certain thruster parameters could be significant. For example, a factor of two increase in neutral temperature would result in a 29% lower neutral density in the chamber than usually assumed. Further improvements in the experimental accuracy of these measurements are required.[41]

Masek[25] has conjectured that chamber walls act as virtual sources of neutrals, based upon studies of modes of propellant injection. That is, neutrals injected into the chamber are presumed to be either specularly reflected or desorbed from chamber walls. In addition, ions undergoing wall recombination eventually leave the walls as neutrals. A calculation of the probability of ionization of neutrals leaving the walls has been made.[42] An expression for the ionization probability per neutral per second has the form

$$P(r,z) = n_o^{-1}(dn_i/dt) \tag{15}$$

where

$$\frac{dn_i}{dt} = n_o n_e \int_0^\infty f(\mathbf{v}_e)\mathbf{v}_e\sigma_+(\mathbf{v}_e)d^3\mathbf{v}_e \tag{16}$$

and n_o is the neutral density, n_i the ion density, n_e the electron density, $\mathbf{v}_e$ the electron speed, $f(\mathbf{v}_e)$ the electron distribution function and $\sigma_+(\mathbf{v}_e)$ the ionization cross section. These expressions are general and must be specialized to include only neutrals leaving the wall. In the reference, an analytical fit to the curve of $P(r,z)$ is given by the expression

$$P(r) = C(\theta)\cos^2(\pi r/2R) \tag{17}$$

where $C(\theta)$ depends upon the angle to the surface normal at which a neutral leaves the wall, and R is the chamber radius. This ionization probability is then used to calculate a percent ionization. It was found that 30% of the neutrals reaching the screen grid at an angle of 45° with the wall normal are ionized. The remaining 70% of these neutrals impinge on the screen grid or are ejected through the grid holes. Calculations of this type for a range of reflection angles θ could possibly be used to calculate total ion production rates and neutral efflux from the thruster.

An interesting method for measuring the neutral efflux density has been presented by Cole et al.[43] The technique consisted of measuring the resonant absorption of the mercury 2537 Å line by neutral Hg atoms in the thruster exhaust. The procedure consists of comparing the beam absorption curves with those obtained from a calibrated absorption cell. Cryogenic baffle and collimaters were used to eliminate stray light and Hg atoms from the source. A light chopper was also used to distinguish the mercury lamp signal from stray light emitted from the chamber. The analytical details of translating the measured absorption data into neutral densities is beyond the scope of the present survey. It will suffice to note that the optically measured propellant utilization efficiencies were within 5% of the gravimetrically measured values.

Ion Chamber Geometry and Magnetic Field Effects

The strong coupling that exists between chamber geometry, magnetic field, and plasma parameters means that varying a parameter such as magnetic field strength can markedly alter the effects of plasma density, electron temperature and plasma potential on thruster performance. An experimental study of this interaction has been performed at Hughes[21] under NASA contract. The thruster parameters varied were magnetic field configuration and strength, discharge chamber length, cathode location and type, the mode of propellant injection, and the beam extraction optics (grid hole size).

Ion chamber diagnostics of various geometries and magnetic field shapes with Langmuir probes were also reported in Ref. 21. An interesting result of these studies was that the fraction open area of the ion optics has a greater effect on improving thruster performance than magnetic field shaping,

although a divergent field was found to be better than a uniform field. Similar conclusions were obtained in an earlier experiment[4] in which the chamber length-to-diameter ratio, hollow cathode baffle position and magnetic field shape were varied. Other probe studies concerning the effect of magnetic field strength on plasma parameters have been reported by Masek.[44] Here the effort was centered on investigating the variations of the electron distribution and plasma parameters (density, temperature, potential) with magnetic field strength. These studies showed an increase in plasma density and electron temperature with field strength, while the plasma potential was found to decrease. Although qualitative explanations for this behavior can be expounded,[44] a more quantitative analysis would require a better understanding of the physical processes of the discharge plasma in a magnetic field.

The most recent experimental study on the effect of chamber geometry and magnetic field shape on discharge chamber performance has been reported by Bechtel.[8] In this study the performance of a 30-cm-diam, hollow cathode thruster was investigated. The chamber geometry and magnetic field shape were optimized concurrently. In addition, improved low specific impulse thruster performance was realized by using a composite (glass-coated) accelerator grid.[45]

Cohen[15] has recently attempted to improve thruster performance by using a multipolar (Ioffe-type) magnetic field configuration to contain electrons. The results indicate, however, that a minimum ev/beam ion is attained that appears to be independent of the field shape.

Summary and Conclusion

This paper presents a survey and evaluation of the present status of research on the discharge chamber of mercury electron bombardment thrusters. One of the major objectives of this research is to provide guidelines for improving thruster performance. In addition, such research increases understanding of the basic physics of gaseous discharges. A list of further experimental studies that are desirable to enhance this understanding is as follows: 1) accurate measurements of the electron energy distribution, 2) measurement of the neutral density in the ion chamber, 3) determination of the effect of metastable states on the energy loss, 4) development of techniques for reducing wall recombination and anode loss, 5) defining a complete set of thruster scaling criteria, and 6) Langmuir probe diagnostics of hollow cathode thrusters.

It would also be useful to have a better theoretical model which would permit the calculation and prediction of thruster performance characteristics. The theoretical models that have been proposed to date to meet this requirement included analyses based on simple continuum equations of a fully ionized plasma, analyses incorporating more complete hydromagnetic equations of motion, and approaches using different forms of the plasma kinetic, or Maxwell-Boltzmann, equation.

For the most part, the simplifications and assumptions needed to make the problem tractable have limited the usefulness of these analyses for estimating thruster performance. However, a recent semiempirical approach for calculations of ion production rates, ion currents, and discharge energy losses appears to yield good agreement with experiment. Although extensive theoretical and experimental effort has been devoted to the plasma of mercury bombardment thrusters, the present survey indicates that our knowledge and understanding of the physics of these plasmas is far from complete.

References

[1] Kaufman, H. R., "An Ion Rocket with an Electron Bombardment Ion Source," TN-D-585, Jan. 1961, NASA.

[2] Sohl, G. et al., "Cesium Electron-Bombardment Ion Microthrusters," *Journal of Spacecraft and Rockets*, Vol. 4, No. 9, Sept. 1967, pp. 1180–1183.

[3] Nakanishi, S. and Pawlik, E. V., "Experimental Investigation of a 1.5 Meter Diameter Kaufman Thrustor," *Journal of Spacecraft and Rockets*, Vol. 5, No. 7, July 1968, pp. 801–807.

[4] Kerslake, W. R., Byers, D. C., and Staggs, J. F., "SERT II Experimental Thrustor System," AIAA Paper 67-700, New York, 1967.

[5] Byers, D. C. and Staggs, J. F., "SERT II Flight-Type Thrustor System Performance," AIAA Paper 69-235, New York, 1969.

[6] Bechtel, R. T., "Discharge Chamber Optimization of the SERT II Thrustor," AIAA Paper 67-668, New York, 1967.

[7] Kerslake, W. R., "Cathode Durability in the Mercury Electron-Bombardment Ion Thrustor," AIAA Paper 64-683, New York, 1964.

[8] Kerslake, W. R., "Preliminary Operation of Oxide-Coated Brush Cathodes in Electron-Bombardment Ion Thrustors," TM X-1105, June 1965, NASA.

[9] Bechtel, R. T., Csiky, G. A., and Byers, D. C., "Performance of a 15-Centimeter Diameter, Hollow-Cathode Kaufman Thrustor," AIAA Paper 68-88, New York, 1968.

[10] Bechtel, R. T., "Performance and Control of a 30-Centimeter Diameter, Low-Impulse Kaufman Thruster," AIAA Paper 69-238, New York, 1969.

[11] Mickelsen, W. R. and Kaufman, H. R., "Electrostatic Thrustors for Space Propulsion, Present and Future," *British Interplanetary Society Journal*, Vol. 19, No. 2, March-April 1964, pp. 319–337, 369–371.

[12] Kerrisk, D. J. and Kaufman, H. R., "Electric Propulsion Systems for Primary Spacecraft Propulsion," AIAA Paper 67-424, New York, 1967.

[13] Richley, E. A. and Kerslake, W. R., "Bombardment Thruster Investigations at the Lewis Research Center," AIAA Paper 68-542, New York, 1968.

[14] Richley, E. A. and Mickelsen, W. R., "Effects of Molecular Flow in Plasma Generation and Some Analyses of Space Charge Flow in Ion Acceleration," AIAA Paper 64-7, New York, 1964.

[15] Cohen, A. J., "An Electron Bombardment Thruster Operated with a Cusped Magnetic Field," TN D-5448, 1969, NASA.

[16] Kohlberg, I. and Nablo, S., "Physical Phenomena in Bombardment Ion Sources," *Physics and Technology of Ion Motors*, edited by F. E. Marble and J. Surugue, Gordon and Breach, New York, 1966, pp. 155–206.

[17] King, H. J. and Kohlberg, I., "Low Current Density Ion Engine Development," Rept. 38TR-102, NASA CR-52440, Jan. 1963, Ion Physics Corp., Burlington, Mass.

[18] Chapman, S. and Cowling, T. G., *The Mathematical Theory of Non-Uniform Gases*, Cambridge Univ. Press, London, 1953.

[19] Kaufman, H. R., "Performance Correlation for Electron-Bombardment Ion Sources," TN D-3041, Oct. 1965, NASA.

[20] Masek, T. D., "Plasma Characteristics of the Electron Bombardment Ion Engine," TR-32-1271, NASA CR-94554, April 1968, Jet Propulsion Lab., California Institute of Technology, Pasadena, Calif.

[21] Knauer, W. et al., "Discharge Chamber Studies for Mercury Bombardment Ion Thrusters," NASA CR-72440, Sept. 1968, Hughes Research Labs., Malibu, Calif.

[22] Cohen, A. J., "Onset of Anomalous Diffusion in Electron-Bombardment Ion Thruster," TN D-3731, Nov. 1966, NASA.

[23] Kadomtsev, B. B. and Nedospasov, A. V., "Instability of the Positive Column in a Magnetic Field and the 'Anomalous' Diffusion Effect," *Journal of Nuclear Energy, Pt. C, Plasma Physics*, Vol. 1, No. 4, 1960, pp. 230–235.

[24] Cohen, A. J., "Anomalous Diffusion in a Plasma Formed from the Exhaust Beam of an Electron-Bombardment Ion Thruster," TN D-4758, Aug. 1968, NASA.

[25] Masek, T. D., "Plasma Properties and Performance of Mercury Ion Thrusters," AIAA Paper 69-256, New York, 1969.

[26] Shaw, E. K., "One- and Two-Dimensional Steady-State Low Pressure Discharge Theory," Rept. ML-1495, NASA CR-54665, Nov. 1966, Microwave Lab., Stanford, Calif.

[27] Tannenbaum, B. S., *Plasma Physics*, McGraw-Hill, New York, 1967, Chap. 4.

[28] Strickfaden, W. B. and Geiler, K. L., "Probe Measurements of the Discharge in an Operating Electron Bombardment Engine," AIAA Paper 63-056, New York, 1963.

[29] Kerrisk, D. J. and Masek, T. D., "Plasma Nonuniformity and Grid Erosion in an Electron Bombardment Ion Engine," *AIAA Journal*, Vol. 3, No. 6, June 1965, pp. 1060–1066.

[30] Medicus, G. K., "A Ball of Fire Discharge with a Pro-

nounced Current Saturation," *Journal Applied Physics*, Vol. 24, No. 2, Feb. 1953, pp. 233–234.

[31] Medicus, G., "On Pronounced Deviations from the Maxwellian Velocity Distribution of the Electrons in Hollow Hot Cathode Diodes with Ne Fillings," *Physical Review*, Vol. 100, No. 4, Nov. 15, 1955, p. 1232.

[32] Masek, T. D. and Kerrisk, D. J., "Plasma Characteristics for Mercury and Cesium Bombardment Ion Engines," *Space Programs Summary 37-32*, Vol. IV, March 31, 1968, Jet Propulsion Lab., California Institute Technology, Pasadena, Calif., pp. 141–148.

[33] Chen, F. F., "Electric Probes," *Plasma Diagnostic Techniques*, edited by R. R. Huddlestone and S. L. Leonard, Academic Press, New York, 1965, p. 137.

[34] Medicus, G., "Simple Way to Obtain the Velocity Distribution of the Electrons in Gas Discharge Plasmas from Probe Curves," *Journal of Applied Physics*, Vol. 27, No. 10, Oct. 1956, pp. 1242–1248.

[35] Dugan, J. V., Jr. and Sovie, R. J., "Volume Ion Production Costs in Tenuous Plasmas: A General Atom Theory and Detailed Results for Helium, Argon, and Cesium," TN D-4150, Sept. 1967, NASA.

[36] Gryzinski, M., "Classical Theory of Electronic and Ionic Inelastic Collisions," *Physical Review*, Vol. 115, No. 2, July 15, 1959, pp. 374–383.

[37] Gryzinski, M., "Classical Theory of Atomic Collisions. I. Theory of Inelastic Collisions," *Physical Review*, Vol. 138, No. 2A, April 19, 1965, pp. 336–358.

[38] Mickelsen, W. R., "Power Loss in Mercury-And-Cesium-Bombardment Thrusters," Advanced Electric Propulsion Research Rept. 6, MER-67-68WRM-9, NASA CR-92560, Dec. 1967, Colorado State Univ., Fort Collins, Colo.

[39] Sovie, R. J. and Dugan, J. V., "Effects of Metastable Atoms on Volume Ion Production in a Tenuous Helium Plasma," TN D-3121, Nov. 1965, NASA.

[40] Staggs, J., Gula, W. P., and Kerslake, W. R., "The Distribution of Neutral Atoms and Charge-Exchange Ions Downstream of an Ion Thruster," AIAA Paper 67-82, New York, 1967.

[41] Mickelsen, W. R., private communication, Jan. 1969, Colorado State Univ., Fort Collins, Colo.

[42] Hodgson, R. T., Fitzgerald, D. C., and Mickelsen, W. R., "Fundamental Plasma Processes in Electron-Bombardment-Thruster Ionization Chambers," Advanced Electric Propulsion Research Report 5, NASA CR-88419, July 1967, College of Engineering, Colorado State Univ., Fort Collins, Colo.

[43] Cole, R. K. et al., "Ion Beam Neutral Component Determinations by Resonance Absorption" AIAA Paper 64-9, New York, 1964.

[44] Masek, T. D., "Plasma Studies in the Electron Bombardment Ion Engine—Magnetic Field Effects," *Space Programs Summary 37-44*, Vol. IV, April 30, 1967, Jet Propulsion Lab., California Institute Technology, Pasadena, Calif., pp. 164–169.

[45] Banks, B., "Composite Ion Accelerator Grids," *Electrochemical Society Third International Conference on Electron and Ion Beam Science and Technology*, Boston, Mass., May 6–9, 1968.